Leukotriene A_4 hydrolase deficiency protects mice from diet-induced obesity by increasing energy expenditure through neuroendocrine axis

Hirotsugu Uzawa, [*, †, 1] Daisuke Kohno, [‡, 1] Tomoaki Koga, [*, §] Tsutomu Sasaki, [‡, ¶] Ayako Fukunaka, [‖] Toshiaki Okuno, [*] Airi Jo-Watanabe, [*] Saiko Kazuno, [#] Takeshi Miyatsuka, [†] Tadahiro Kitamura, [‡] Yoshio Fujitani, [‖] Hirotaka Watada, [†] Kazuko Saeki, [*, 2] and Takehiko Yokomizo, [*]

[*] Department of Biochemistry, Graduate School of Medicine, Juntendo University, Bunkyo-ku, Tokyo, Japan

[†] Department of Metabolism and Endocrinology, Graduate School of Medicine, Juntendo University, Bunkyo-ku, Tokyo, Japan

[‡] Metabolic Signal Research Center, Institute for Molecular and Cellular Regulation, Gunma University, Maebashi-city, Gunma, Japan

[§] Department of Medical Cell Biology, Institute of Molecular Embryology and Genetics, Kumamoto University, Chuo-ku, Kumamoto, Japan

[¶] Division of Food Science and Biotechnology, Graduate School of Agriculture, Kyoto University, Sakyo-ku, Kyoto, Japan

[‖] Laboratory of Developmental Biology and Metabolism, Institute for Molecular and Cellular Regulation, Gunma University, Maebashi-city, Gunma, Japan

[#] Laboratory of Proteomics and Biomolecular Science, Research Support Center, Juntendo University Graduate School of Medicine, Bunkyo-ku, Tokyo, Japan

[1] These authors contributed equally.

[2] Correspondence: Department of Biochemistry, Juntendo University Graduate School of Medicine, Hongo 2-1-1, Bunkyo-ku, Tokyo 113-8421, Japan.

Email: ksaeki@juntendo.ac.jp

Telephone: +81-3-5802-1031

Fax: +81-3-5802-5889

short/running title: LTA_4H protects mice from diet-induced obesity

Abbreviations: BAT, Brown adipose tissue; BMI, body mass index; HFD, high-fat diet; LTA_4H, leukotriene A_4 hydrolase; LTB_4, leukotriene B_4; SD, standard diet; SVF, stromal vascular fraction; UCP1, uncoupling protein 1

Summary

Obesity is a health problem worldwide, and brown adipose tissue (BAT) is important for energy expenditure. Here, we explored the role of leukotriene A_4 hydrolase (LTA_4H), a key enzyme in the synthesis of the lipid mediator leukotriene B_4 (LTB_4), in diet-induced obesity. LTA_4H-deficient (LTA_4H-KO) mice fed a high-fat diet (HFD) showed a lean phenotype, and bone-marrow transplantation studies revealed that LTA_4H-deficiency in non-hematopoietic cells was responsible for this lean phenotype. LTA_4H-KO mice exhibited greater energy expenditure, but similar food intake and fecal energy loss. LTA_4H-KO BAT showed higher expression of thermogenesis-related genes. In addition, the plasma thyroid-stimulating hormone and thyroid hormone concentrations, as well as HFD-induced catecholamine secretion, were higher in LTA_4H-KO mice. By contrast, LTB_4 receptor (BLT1)-deficient mice did not show a lean phenotype, implying that the phenotype of LTA_4H-KO mice is independent of the LTB_4/BLT1 axis. These results indicate that LTA_4H mediates diet-induced obesity by reducing catecholamine and thyroid hormone secretion.

Keywords

brown adipocyte, uncoupling protein 1, thyroid hormone, noradrenaline, peptidase

Introduction

Obesity is now a pandemic. According to the World Health Organization, more than 1 billion adults (about 15% of the world population) are overweight (body mass index [BMI] > 25 kg/m^2), and more than 300 million are classified as obese (BMI > 30 kg/m^2). Obesity represents a major risk factor for the development of many of the most common diseases, including type 2 diabetes mellitus, dyslipidemias, non-alcoholic fatty liver disease, cardiovascular disease, Alzheimer's disease, and some cancers (1). Therefore, there is a great need for strategies for the prevention and treatment of overweight and obesity. There are various ways of losing weight, including reducing food intake, reducing the intestinal absorption of nutrients, and increasing energy expenditure. Brown adipose tissue (BAT) is a metabolically active tissue that contributes to energy expenditure. Specifically, it dissipates stored chemical energy in the form of heat, its mass inversely correlates with BMI, and it is considered to have an anti-obesity role (2, 3). Therefore, the activation of BAT might permit the maintenance or loss of body mass, even if individuals continue to consume a lipid-rich diet (4). Uncoupling protein 1 (UCP1) is essential for thermogenesis in both brown and beige adipocytes (5), and its activity contributes to the regulation of energy balance (6). A few reports are available for understanding the relationship between lipid mediators and metabolism. These reports show that some lipid mediators regulate glucose tolerance and insulin resistance through inflammation in metabolic tissues, such as liver and adipose tissue (7, 8). However, there are few reports about the role of lipid mediators on obesity (9).

Our laboratory has been working on the *in vivo* roles of lipid mediators for a long time, especially leukotriene B_4 (LTB_4). LTB4 is produced by leukotriene A4 hydrolase (LTA_4H) from arachidonic acid in hematopoietic cells, and exerts its effects by binding to the high-affinity LTB_4 receptor (BLT1) (10). BLT1 is expressed in inflammatory leukocytes such as neutrophils, eosinophils, effector T-cells, and subsets of macrophages and dendritic cells, and it plays important roles in inflammation (11). During the early phase of inflammation, LTB_4 is generated by LTA_4H in activated leukocytes and attracts other leukocytes, which express BLT1, to sites of inflammation. In relation to metabolism, LTB_4/BLT1 axis promotes inflammation in adipose tissue, liver, and skeletal muscle in

mice (12, 13). Although there have been many studies of the roles of BLT1 and LTB_4, which used BLT1 antagonists and BLT1-deficient (BLT1-KO) mice, only a few *in vivo* studies of the roles of LTA_4H have been conducted (14, 15). LTA_4H is expressed not only in hematopoietic cells but also in the other cells than hematopoietic cells. LTA_4H-deficient (LTA_4H-KO) mice, which were generated as early as 1999, used in an experimental model of peritonitis, and there was not reported in metabolic phenotype (16). As we are interested in the relationship between LTA_4H and metabolism, we originally generated LTA_4H-KO mice on C57BL/6 background and found the lean phenotype of this mouse. Here, we clarified the roles of LTA_4H in a high-fat diet (HFD)-induced obesity. Our experiments unveiled the significant relationship between LTA_4H and metabolism, which might help us to develop novel therapeutic methods for obesity.

Materials and Methods

Mice

BLT1-KO (*Ltb4r1*$^{-/-}$) mice were generated as previously described (17). LTA_4H-KO (*Lta4h*$^{-/-}$) mice were generated using the CRISPR/Cas9 system on a C57BL/6 background and the details will be reported in another paper (Koga et al., submitted). All experiments were performed using male mice. LTA_4H-KO and BLT1-KO mice were compared with their WT littermates. The mice were housed with free access to food (SD; CRF-1 [Oriental Yeast, Itabashi, Tokyo, Japan] or a 60% HFD [D12492; Research Diets, NJ, USA]) and drinking water in a specific pathogen-free facility. The body mass of the LTA_4H-KO and BLT1-KO mice was measured every week. All animal experiments were approved by the Ethics Committees for Animal Experiments of Juntendo University School of Medicine, and were performed according to appropriate guidelines and regulations.

Measurement of food intake

Mice at 7 weeks of age were acclimated to the use of multi-feeders (Shinfactory, Higashi, Fukuoka, Japan) for 1 week. Food intake was measured daily. During this measurement period, mice were housed in individual cages.

Measurement of the nutrient energy in feces

Dried feces from mice fed the HFD were collected and used to measure the residual nutrient energy content by direct calorimetry at the Chemicals Evaluation and Research Institute, Japan.

Histological analysis

Mouse tissues were dissected, rinsed with phosphate-buffered saline (PBS), fixed in 4% formaldehyde or paraformaldehyde in phosphate buffer, and embedded in paraffin blocks. Tissue sections (4 μm thickness) were stained with H&E.

Body composition analysis using micro-computed tomography (CT)

CT was performed under isoflurane anesthesia using a LaTheta micro-CT scanner (Hitachi, Chiyoda, Tokyo, Japan). The abdominal region between the first and sixth lumbar vertebrae was scanned, and the sizes of the fat and soft tissue compartments were measured.

Indirect calorimetry

VO_2 and VCO_2 were measured in individual mice at the indicated ages using an Oxymax apparatus (Columbus Instruments, Columbus, OH, USA). The O_2 and CO_2 measurements were performed every 18 min over a 3-day period, during both the light and dark phases, and the data from the final day were analyzed.

Measurement of lipid droplet area in the liver and BAT

The size of the lipid droplets (μm^2) was measured using ImageJ software (NIH, Bethesda, MD, USA).

qRT-PCR

RNA was extracted using TRIzol reagent (Invitrogen, Carlsbad, CA, USA), and cDNA was synthesized using the QuantiTect Reverse Transcription Kit (Qiagen, Hilden, Nordrhein-Westfalen, GER). Real-time PCR analysis was performed using the LightCycler 96 (Roche Diagnostics, Indianapolis, IN, USA) and FastStart Essential DNA Green Master Mix (Roche Diagnostics), according to the manufacturer's protocol. The sequences of primers used are listed in **Supplemental Table S1**.

Bone marrow transplantation studies

Bone marrow cells were collected from the femora, tibiae, and humeri of donor mice, and mature T-lymphocytes were depleted in these using biotinylated anti-CD5 antibody (BioLegend, San Diego, CA, USA) and streptavidin beads (Miltenyi Biotec, Bergisch Gladbach, Nordrhein-Westfalen, GER), to prevent acute graft-versus-host disease. Recipient mice (7–10 weeks of age) were irradiated (9 Gy) and transplanted with 6.5–8.0 × 10^6 of these bone marrow cells by injection into the retro-orbital venous plexus.

Subsequently, the mice were fed the SD until they were 15 weeks of age, and then from 15 to 27 weeks of age they were fed the HFD and were weighed every week.

Separation of the SVF from BAT and its differentiation to yield brown adipocytes

Interscapular BAT was excised from mice, minced with scissors, suspended in 10 mL PBS containing 1.5 U/mL collagenase D and 2.4 U/mL dispase II, and digested at 37°C, with constant agitation at 150 rpm for 40 min. The cell suspension was then filtered through a 70 μm cell strainer and centrifuged at 700 × *g* for 10 min. The cell pellet (the SVF) was re-suspended in 10 mL DMEM/F12 (Gibco, Carlsbad, CA, USA) containing 10% fetal bovine serum (FBS), seeded into a collagen-coated 10 cm dish (Iwaki, Haibara, Shizuoka, Japan), and incubated for 5 days. The cells were then detached and seeded into a collagen-coated 12-well plate (1.6×10^5 cells/well) and differentiated into brown adipocytes by incubation in induction medium (DMEM/F12 medium containing 10% FBS, 100 U/mL penicillin, 100 μg/mL streptomycin, 861 nM insulin, 1 nM T3, 125 μM indomethacin, 2 μg/mL dexamethasone, 500 μM isobutylmethylxanthine, and 0.5 μM rosiglitazone) for 2 days, followed by incubation in maintenance medium (DMEM/F12 medium containing 10% FBS, 100 U/mL penicillin, 100 μg/mL streptomycin, 861 nM insulin, 1 nM T3, and 0.5 μM rosiglitazone) for a further 2 days. The cells were then maintained in a medium containing a high concentration of rosiglitazone (DMEM/F12 medium containing 10% FBS, 100 U/mL penicillin, 100 μg/mL streptomycin, 861 nM insulin, 1 nM T3, and 1 μM rosiglitazone) for 3 days. Seven days after the start of the differentiation process, fully differentiated brown adipocytes were stimulated with 10 μM isoproterenol for 1, 6, or 24 hours.

Measurement of urine catecholamine concentration

Twenty-four-hour urine collection was performed using bottles containing 1.2 mL of 1N HCl. The collected samples were filled up to 3 mL with deionized water and stored at −80°C until analysis. Urinary catecholamine concentration was measured using high-performance liquid chromatography at the Japan Institute for the Control of Aging, Nikken SEIL Co., Ltd.

Measurement of plasma thyroid hormone concentration

The plasma concentrations of TSH, T3, and T4 were measured using a Milliplex thyroid hormone panel kit (Millipore, Billerica, MA, USA) and a Luminex 200 analyzer (Millipore).

Flow cytometry

Peripheral blood leukocytes from WT and LTA_4H-KO mice (Ly 5.2) transplanted with WT bone marrow cells (Ly 5.1) were stained with allophycocyanin (APC)-conjugated anti-CD 45.1 and phycoerythrin (PE)-conjugated anti-CD 45.2 antibodies. These cells were analyzed using a CytoFLEX flow cytometer (Beckman Coulter, Brea, CA, USA), and the data were analyzed using FlowJo software (Becton, Dickinson, Franklin Lakes, NJ, USA).

Statistical analysis

All data were analyzed using GraphPad Prism software (GraphPad, San Diego, CA, USA). The statistical tests used for each analysis are listed in the respective figure legends.

Data and code availability

This study did not generate datasets or codes.

Results

LTA_4H deficiency protects mice from high-fat diet-induced obesity

To investigate the roles of LTA_4H in metabolism, we first monitored the growth of wild-type (WT) and LTA_4H-KO mice. Because LTA_4H-KO mice showed a slightly lean phenotype compared with their WT littermates while eating a standard diet (SD) **(Fig. 1A)**, we challenged a group of mice with the HFD after weaning (4 weeks of age). Whereas WT mice showed obvious gains in body mass, these gains were significantly lower in LTA_4H-KO mice **(Fig. 1A)**. Next, we determined the effect of LTA_4H deficiency in metabolic tissues. In 27-week-old mice, HFD-induced liver hypertrophy was ameliorated by LTA_4H-deficiency **(Fig. 1B, C)**. We analyzed the histology of the liver and BAT of LTA_4H-KO mice, and found that there were smaller lipid droplets in the liver and BAT in LTA_4H-KO mice than in WT mice **(Fig. 1D, E)**. We next evaluated the body composition of 12-week-

old mice using micro-CT. There was no significant difference in adipose tissue weight, and body fat percentage between LTA_4H-KO and WT mice fed the SD **(Fig. 1F)**. Therefore, we challenged a group of mice with the HFD and found that 12-week-old LTA_4H-KO mice were slightly leaner than WT mice of the same age when they had been fed the HFD. Whereas the lean body masses of LTA_4H-KO and WT mice were comparable, the body fat percentage of LTA_4H-KO mice was lower than that of WT mice **(Fig. 1G)**.

LTA_4H deficiency protects mice from diet-induced obesity by stimulating energy expenditure

To determine whether the lean phenotype of the LTA_4H-KO mice is due to lower food intake, we compared the food intake of HFD-fed LTA_4H-KO and WT mice for 3 weeks, and found that there was no difference **(Fig. 2A)**. We also measured the energy lost in the feces, and found that this was comparable between LTA_4H-KO and WT mice **(Fig. 2B)**. In addition, we performed histological analysis of the small intestine, and found no detectable morphological differences between WT and LTA_4H-KO mice **(Fig. 2C)**. Therefore, we concluded that the lean phenotype of the LTA_4H-KO mice is not due to lower food intake or nutrient absorption. We next hypothesized that the lean phenotype might be the result of higher energy expenditure. To test this hypothesis, we evaluated the basal metabolism of LTA_4H-KO mice. We found no significant difference in energy expenditure assessed using oxygen consumption (VO_2) and carbon dioxide production (VCO_2), between LTA_4H-KO and WT mice fed the SD **(Fig. 2D)**. On the other hand, the levels of VO_2, VCO_2, and locomotor activity of LTA_4H-KO mice were higher than those of WT mice fed the HFD **(Fig. 2E)**. These results suggest that LTA_4H deficiency protects mice from diet-induced obesity by increasing energy expenditure.

LTA_4H deficiency stimulates BAT thermogenesis through neuroendocrine axis

According to the results of a previous study (18) and NCBI database (https://www.ncbi.nlm.nih.gov/gene?Db=gene&Cmd=DetailsSearch&Term=16993), LTA_4H is ubiquitously expressed, but its expression is particularly high in hematopoietic cells. We found that LTA_4H is also highly expressed in lymphoid organs, such as spleen

and intestine, and that it is expressed in metabolic tissues, such as BAT **(Supplemental Fig. S1)**. To determine which LTA_4H-expressing cells contribute to the metabolic phenotype, we performed a bone marrow transplantation study. LTA_4H-KO mice that received WT bone marrow exhibited lower body mass gain upon the HFD feeding **(Fig. 3A)**, whereas the body mass gains of recipient mice transplanted with WT or LTA_4H-deficient bone marrow were comparable **(Fig. 3B)**. The body mass data are shown in **Supplemental Fig. S2A, B**. Approximately 95% of the bone marrow was replaced in each case **(Supplemental Fig. S2C)**. These results show that LTA_4H in non-hematopoietic cells contributes to the metabolic phenotype. BAT is well known to be a diet-induced thermogenic tissue; therefore, we measured the expression of thermogenesis-related genes in the BAT of LTA_4H-KO mice. The expression of brown adipocyte-specific markers, such as *Ucp1*, *Ppara*, *Cidea*, and *Pgc1b*, in BAT was higher in LTA_4H-KO than in WT mice **(Fig. 3C)**, but the expression of adipocyte-specific markers, such as *Adipoq*, in epididymal white adipose tissue (eWAT) did not differ between the sets of mice (data not shown). These data suggest that the thermogenic activity of BAT is higher in LTA_4H-KO mice fed the HFD than in WT mice, which may explain the lean phenotype of the LTA_4H-KO mice. The *Ucp1* expression in BAT was also higher in young LTA_4H-KO mice (12 weeks of age) fed the HFD, but not in those fed the SD **(Fig. 3D)**. These data indicate that LTA_4H deficiency increases BAT metabolism in response to the HFD feeding. We next isolated the stromal vascular fraction (SVF) of the BAT from LTA_4H-KO and WT mice, induced its differentiation into brown adipocytes, and measured the expression of thermogenesis-related genes. We found no differences in the expression of *Pparg*, *Nd1*, and *Cox1* between primary brown adipocytes derived from LTA_4H-KO and WT mice **(Fig. 3E)**, which indicates that LTA_4H-deficiency does not affect the differentiation of brown adipocytes. To evaluate the responsiveness of primary brown adipocytes to a beta-adrenergic receptor agonist, we quantified the expression of the thermogenesis-related gene *Ucp1* before and after stimulation with the non-selective beta-agonist isoproterenol. We found no difference in isoproterenol-induced *Ucp1* expression between LTA_4H-deficient and WT brown adipocytes **(Fig. 3F)**. These results suggest that the high expression of thermogenesis-related genes in LTA_4H-deficient BAT *in vivo* is not a brown adipocyte-autonomous

phenomenon. Next, we compared the concentrations of hormones with metabolic effects in the plasma and urine of WT and LTA_4H-KO mice. In particular, pituitary and thyroid hormones, and catecholamines, are known to increase *Ucp1* expression in BAT (19). The plasma thyroid-stimulating hormone (TSH) and thyroxine (T4) concentrations in LTA_4H-KO mice were higher than those in WT mice, but the plasma triiodothyronine (T3) concentrations were comparable **(Fig. 3G)**. These results suggest that LTA_4H deficiency is associated with higher TSH secretion, which stimulates the release of T4, causing the greater energy expenditure. Next, we compared the effect of switching the mice from the SD to HFD on their urinary noradrenaline concentration, and found that this was greater in LTA_4H-KO mice **(Fig. 3H)**. Catecholamine secretion from the adrenal gland is regulated by sympathetic nerves; therefore, these findings suggest that greater energy expenditure in LTA_4H-KO mice may be caused by greater secretion of adrenal hormones, secondary to sympathetic nerve activation.

LTA_4H deficiency protects mice from diet-induced obesity independently of LTB_4/BLT1 axis

To determine whether this lean phenotype is caused by defective LTB_4 synthesis and a resultant reduction in BLT1 activation, we monitored the growth of WT and BLT1-KO mice. To our surprise, the BLT1-KO mice did not show a lean phenotype under either the SD or HFD fed conditions **(Fig. 4A)**. We could not find any significant difference in liver and BAT between BLT1-KO and WT mice. **(Fig. 4B, C)**. Furthermore, there was no significant difference in body composition between HFD-fed BLT1-KO and WT mice **(Fig. 4D)**. These data indicate that the lean phenotype of the LTA_4H-KO mice is not dependent on the LTB_4/BLT1 axis.

Discussion

In contrast to the numerous reports on the phenotypes of BLT1-KO mice in various disease models (11, 20), almost nothing is known about *in vivo* roles of LTA_4H. The study of LTA_4H commenced with protein purification and cDNA cloning as early as the 1980s (15, 21). LTA_4H-KO mice were reported to exhibit milder peritonitis than WT mice following zymosan A injection in 1999, but no further investigations were conducted until 2010. In addition to its LTB_4 biosynthetic activity, LTA_4H has an aminopeptidase activity that was demonstrated using synthetic peptides (22-24). However, the endogenous substrate for this aminopeptidase activity was not identified for a long time. Snelgrove et al. reported that acute lung injury in LTA_4H-KO mice is exacerbated by impaired degradation of the collagen-derived inflammatory peptide proline-glycine-proline (PGP), which suggested that PGP is an endogenous substrate of the LTA_4H aminopeptidase (25, 26). However, these studies used LTA_4H-KO mice on a 129/SvEv background, which is not suitable for the study of various disease models. Therefore, we created LTA_4H-KO C57BL/6 mice for the study of the *in vivo* roles of LTA_4H (Koga et al., submitted). During the maintenance of these LTA_4H-KO mice, we noticed that aged LTA_4H-KO mice were slightly leaner than their WT littermates, which prompted us to analyze the roles of LTA_4H in metabolism.

This is the first study to show the involvement of LTA_4H in diet-induced obesity. Because the lean phenotype of LTA_4H-KO mice was not observed in BLT1-KO mice, we hypothesized that the aminopeptidase activity of LTA_4H is important in diet-induced obesity, and we tried to generate mice that were deficient only in the aminopeptidase activity of LTA_4H. According to previous reports, the amino acid residue Glu-297 of LTA_4H is crucial for its aminopeptidase activity but not for its LTB_4-synthesizing activity. *In vitro* studies showed that the LTA_4H mutant E297Q was still capable of generating LTB_4 but did not possess an aminopeptidase activity (27, 28). Therefore, we established two lines of LTA_4H E297Q-knock in (LTA_4H E297Q-KI) mice to determine the roles of the LTA_4H aminopeptidase activity *in vivo*. We were able to confirm the loss of the aminopeptidase activity of LTA_4H in these LTA_4H-KI mice and to reproduce the lean phenotype (data not shown). However, the LTB_4 synthesis in the bone marrow-derived dendritic cells (BMDCs) from these LTA_4H-KI mice was only 10% of that in WT BMDCs (data not shown), and

331 therefore we could not conclude that the loss of the aminopeptidase activity of LTA$_4$H is
332 responsible for the lean phenotype of the LTA$_4$H-KO and LTA$_4$H E297Q-KI mice.
333 LTA$_4$H deficiency resulted in an amelioration of HFD-induced obesity, which was
334 accompanied by greater energy expenditure and higher expression of thermogenesis-related
335 genes. A bone marrow transplantation experiment showed that LTA$_4$H expression in non-
336 hematopoietic cells is responsible for this metabolic phenotype. We next measured the
337 expression of LTA$_4$H in various tissues in mice, and found the highest level of expression
338 in the spleen and intestine, followed by BAT **(Supplemental Fig. S1)**. Therefore, we
339 explored the roles of LTA$_4$H in BAT using LTA$_4$H-KO mice. We isolated the SVF from
340 interscapular BAT, differentiated the cells into brown adipocytes *in vitro*, and measured the
341 expression of brown adipocyte differentiation markers and the response to catecholamines.
342 The expression of brown adipocyte differentiation markers (*Pparg*, *Nd1*, and *Cox1*) and the
343 isoproterenol-induced upregulation of *Ucp1* mRNA were comparable between WT and
344 LTA$_4$H-KO mice **(Fig. 3E, F)**. Because an analysis of brown adipocytes alone could not
345 explain the difference in phenotype between the WT and LTA$_4$H-KO mice, we measured
346 the concentrations of several hormones that regulate energy expenditure in BAT. The
347 plasma concentrations of TSH and T4 were higher in LTA$_4$H-KO than in WT mice **(Fig.**
348 **3G)**, and the secretion of noradrenaline was greater in HFD-fed LTA$_4$H-KO than WT mice
349 **(Fig. 3H)**. Although LTA$_4$H is expressed in the hypothalamus, pituitary, thyroid, and
350 adrenal gland (https://www.proteinatlas.org/ENSG00000111144-LTA4H/tissue), no reports
351 are available on the relationship between the neuroendocrine axis and LTA$_4$H. Elevated
352 levels of TSH, T4, and noradrenaline can explain the lean phenotype of LTA$_4$H-KO mice.
353 In summary, we identified a novel role for LTA$_4$H in metabolism, although the
354 detailed molecular mechanism involved has yet to be determined. Considering the fact that
355 this enzyme is widely expressed in tissues and cells, there are several experiments that
356 would provide additional information regarding its roles in metabolism and energy
357 expenditure. First, the generation of cell type-specific LTA$_4$H-KO mice would be of
358 interest. Second, a denervation study to clarify the relationships between the thyroid gland,
359 adrenal gland, and sympathetic nerves would also clarify the mechanisms involved. Third,
360 experiments aimed at determining the roles of the aminopeptidase activity of LTA$_4$H in

obesity would be of great interest. LTA_4H inhibitors are currently being developed (29-31), and LTA_4H inhibition might increase HFD-induced thermogenesis, which would make it a promising therapeutic target for obesity.

Acknowledgments

We thank the Laboratories of Proteomics and Biomolecular Science, Morphology and Image Analysis, Biomedical Research Resources, and Molecular and Biochemical Research at Juntendo University for technical support. This work was carried out by the Joint Research Program of the Institute for Molecular and Cellular Regulation, Gunma University. This work was supported by MEXT/JSPS KAKENHI grants (nos. JP18K06923 [to KS], JP17K08664 [to TKoga], JP19K07357 [to TO], JP18K15051 [to AJ], and JP15H05904, JP15H05897, JP18H02627, and JP19KK0199 [to TY]); AMED-CREST (no. JP20gm1210006); the Ono Medical Research Foundation; the Takeda Science Foundation; a Grant-in-Aid (no. S1311011) from the Foundation of Strategic Research Projects in Private Universities from the MEXT; and an Institutional Grant for Environmental and Gender-Specific Medicine to Juntendo University School of Medicine. The authors declare no competing interests.

Author contributions

H. Uzawa, K. Saeki, T. Koga, T. Miyatsuka, T. Kitamura, Y. Fujitani, H. Watada, and T. Yokomizo designed the experiments. H. Uzawa, K. Saeki, D. Kohno, T. Koga, A. Fukunaka, T. Sasaki, and T. Okuno performed the experiments. H. Uzawa, K. Saeki, D. Kohno, T. Koga, T. Sasaki, A. Jo, and S. Kazuno analyzed the data. H. Uzawa, K. Saeki, and T. Yokomizo wrote the manuscript.

References

1. Tseng, Y. H., Cypess, A. M., and Kahn, C. R. (2010) Cellular bioenergetics as a target for obesity therapy. *Nat Rev Drug Discov* **9**, 465-482
2. van Marken Lichtenbelt, W. D., Vanhommerig, J. W., Smulders, N. M., Drossaerts, J. M. A. F. L., Kemerink, G. J., Bouvy, N. D., Schrauwen, P., and Teule, G. J. J. (2009) Cold-Activated Brown Adipose Tissue in Healthy Men. *N. Engl. J. Med.* **360**, 1500-1508
3. Virtanen, K. A., Lidell, M. E., Orava, J., Heglind, M., Westergren, R., Niemi, T., Taittonen, M., Laine, J., Savisto, N.-J., Enerbäck, S., and Nuutila, P. (2009) Functional Brown Adipose Tissue in Healthy Adults. *N. Engl. J. Med.* **360**, 1518-1525
4. Stock, M. J. (1989) The role of brown adipose tissue in diet-induced thermogenesis. *Proc. Nutr. Soc.* **48**, 189-196
5. Golozoubova, V., Hohtola, E., Matthias, A., Jacobsson, A., Cannon, B., and Nedergaard, J. (2001) Only UCP1 can mediate adaptive nonshivering thermogenesis in the cold. *FASEB Journal* **15**, 2048-2050
6. Feldmann, H. M., Golozoubova, V., Cannon, B., and Nedergaard, J. (2009) UCP1 ablation induces obesity and abolishes diet-induced thermogenesis in mice exempt from thermal stress by living at thermoneutrality. *Cell Metab.* **9**, 203-209
7. Yasui, M., Tamura, Y., Minami, M., Higuchi, S., Fujikawa, R., Ikedo, T., Nagata, M., Arai, H., Murayama, T., and Yokode, M. (2015) The Prostaglandin E2 Receptor EP4 Regulates Obesity-Related Inflammation and Insulin Sensitivity. *PLoS One* **10**, e0136304

8. Syed, I., Lee, J., Moraes-Vieira, P. M., Donaldson, C. J., Sontheimer, A., Aryal, P., Wellenstein, K., Kolar, M. J., Nelson, A. T., Siegel, D., Mokrosinski, J., Farooqi, I. S., Zhao, J. J., Yore, M. M., Peroni, O. D., Saghatelian, A., and Kahn, B. B. (2018) Palmitic Acid Hydroxystearic Acids Activate GPR40, Which Is Involved in Their Beneficial Effects on Glucose Homeostasis. *Cell Metab.* **27**, 419-427 e414

9. Fujimori, K., Aritake, K., Oishi, Y., Nagata, N., Maehara, T., Lazarus, M., and Urade, Y. (2019) L-PGDS-produced PGD2 in premature, but not in mature, adipocytes increases obesity and insulin resistance. *Sci Rep* **9**, 1931

10. Yokomizo, T., Izumi, T., Chang, K., Takuwa, Y., and Shimizu, T. (1997) A G-protein-coupled receptor for leukotriene B4 that mediates chemotaxis. *Nature* **387**, 620-624

11. Yokomizo, T., Nakamura, M., and Shimizu, T. (2018) Leukotriene receptors as potential therapeutic targets. *J. Clin. Invest.* **128**, 2691-2701

12. Li, P., Oh, D. Y., Bandyopadhyay, G., Lagakos, W. S., Talukdar, S., Osborn, O., Johnson, A., Chung, H., Maris, M., Ofrecio, J. M., Taguchi, S., Lu, M., and Olefsky, J. M. (2015) LTB4 promotes insulin resistance in obese mice by acting on macrophages, hepatocytes and myocytes. *Nat. Med.* **21**, 239-247

13. Spite, M., Hellmann, J., Tang, Y., Mathis, S. P., Kosuri, M., Bhatnagar, A., Jala, V. R., and Haribabu, B. (2011) Deficiency of the leukotriene B4 receptor, BLT-1, protects against systemic insulin resistance in diet-induced obesity. *J. Immunol.* **187**, 1942-1949

14. Haeggström, J. Z. (2018) Leukotriene biosynthetic enzymes as therapeutic targets. *Journal of Clinical Investigation* **128**, 2680-2690

15. Minami, M., Ohno, S., Kawasaki, H., Radmark, O., Samuelsson, B., Jornvall, H., Shimizu, T., Seyama, Y., and Suzuki, K. (1987) Molecular cloning of a cDNA coding for human leukotriene A4 hydrolase. Complete primary structure of an enzyme involved in eicosanoid synthesis. *J. Biol. Chem.* **262**, 13873-13876

16. Byrum, R. S., Goulet, J. L., Snouwaert, J. N., Griffiths, R. J., and Koller, B. H. (1999) Determination of the Contribution of Cysteinyl Leukotrienes and Leukotriene B4 in

438 Acute Inflammatory Responses Using 5-Lipoxygenase- and Leukotriene A4
439 Hydrolase-Deficient Mice. *J. Immunol.* **163**, 6810-6819
440 17. Terawaki, K., Yokomizo, T., Nagase, T., Toda, A., Taniguchi, M., Hashizume, K.,
441 Yagi, T., and Shimizu, T. (2005) Absence of leukotriene B4 receptor 1 confers
442 resistance to airway hyperresponsiveness and Th2-type immune responses. *J.*
443 *Immunol.* **175**, 4217-4225
444 18. Ohishi, N., Minami, M., Kobayashi, J., Seyama, Y., Hata, J., Yotsumoto, H., Takaku,
445 F., and Shimizu, T. (1990) Immunological quantitation and immunohistochemical
446 localization of leukotriene A4 hydrolase in guinea pig tissues. *J. Biol. Chem.* **265**,
447 7520-7525
448 19. Bianco, A. C., and McAninch, E. A. (2013) The role of thyroid hormone and brown
449 adipose tissue in energy homoeostasis. *The Lancet Diabetes & Endocrinology* **1**, 250-
450 258
451 20. Saeki, K., and Yokomizo, T. (2017) Identification, signaling, and functions of LTB4
452 receptors. *Semin. Immunol.* **33**, 30-36
453 21. Fitzpatrick, F., Haeggstrom, J., Granstrom, E., and Samuelsson, B. (1983)
454 Metabolism of leukotriene A4 by an enzyme in blood plasma: a possible leukotactic
455 mechanism. *Proc. Natl. Acad. Sci. U. S. A.* **80**, 5425-5429
456 22. Toh, H., Minami, M., and Shimizu, T. (1990) Molecular evolution and zinc ion
457 binding motif of leukotriene A4 hydrolase. *Biochem. Biophys. Res. Commun.* **171**,
458 216-221
459 23. Orning, L., Gierse, J. K., and Fitzpatrick, F. A. (1994) The bifunctional enzyme
460 leukotriene-A4 hydrolase is an arginine aminopeptidase of high efficiency and
461 specificity. *J. Biol. Chem.* **269**, 11269-11273
462 24. Tholander, F., Muroya, A., Roques, B. P., Fournie-Zaluski, M. C., Thunnissen, M.
463 M., and Haeggstrom, J. Z. (2008) Structure-based dissection of the active site
464 chemistry of leukotriene A4 hydrolase: implications for M1 aminopeptidases and
465 inhibitor design. *Chem. Biol.* **15**, 920-929
466 25. Snelgrove, R. J., Jackson, P. L., Hardison, M. T., Noerager, B. D., Kinloch, A.,
467 Gaggar, A., Shastry, S., Rowe, S. M., Shim, Y. M., Hussell, T., and Blalock, J. E.

(2010) A critical role for LTA4H in limiting chronic pulmonary neutrophilic inflammation. *Science* **330**, 90-94

26. Akthar, S., Patel, D. F., Beale, R. C., Peiro, T., Xu, X., Gaggar, A., Jackson, P. L., Blalock, J. E., Lloyd, C. M., and Snelgrove, R. J. (2015) Matrikines are key regulators in modulating the amplitude of lung inflammation in acute pulmonary infection. *Nat. Commun.* **6**, 8423

27. Minami, M., Bito, H., Ohishi, N., Tsuge, H., Miyano, M., Mori, M., Wada, H., Mutoh, H., Shimada, S., Izumi, T., and et al. (1992) Leukotriene A4 hydrolase, a bifunctional enzyme. Distinction of leukotriene A4 hydrolase and aminopeptidase activities by site-directed mutagenesis at Glu-297. *FEBS Lett.* **309**, 353-357

28. Wetterholm, A., Medina, J. F., Radmark, O., Shapiro, R., Haeggstrom, J. Z., Vallee, B. L., and Samuelsson, B. (1992) Leukotriene A4 hydrolase: abrogation of the peptidase activity by mutation of glutamic acid-296. *Proc. Natl. Acad. Sci. U. S. A.* **89**, 9141-9145

29. Stsiapanava, A., Olsson, U., Wan, M., Kleinschmidt, T., Rutishauser, D., Zubarev, R. A., Samuelsson, B., Rinaldo-Matthis, A., and Haeggstrom, J. Z. (2014) Binding of Pro-Gly-Pro at the active site of leukotriene A4 hydrolase/aminopeptidase and development of an epoxide hydrolase selective inhibitor. *Proc. Natl. Acad. Sci. U. S. A.* **111**, 4227-4232

30. König, S., Pace, S., Pein, H., Heinekamp, T., Kramer, J., Romp, E., Straßburger, M., Troisi, F., Proschak, A., Dworschak, J., Scherlach, K., Rossi, A., Sautebin, L., Haeggström, J. Z., Hertweck, C., Brakhage, A. A., Gerstmeier, J., Proschak, E., and Werz, O. (2019) Gliotoxin from Aspergillus fumigatus Abrogates Leukotriene B4 Formation through Inhibition of Leukotriene A4 Hydrolase. *Cell Chemical Biology* **26**, 524-534.e525

31. Low, C. M., Akthar, S., Patel, D. F., Loser, S., Wong, C. T., Jackson, P. L., Blalock, J. E., Hare, S. A., Lloyd, C. M., and Snelgrove, R. J. (2017) The development of novel LTA4H modulators to selectively target LTB4 generation. *Sci Rep* **7**, 44449

Figure legends

Figure 1. LTA$_4$H deficiency protects mice from diet-induced obesity. A) Growth curve of LTA$_4$H-KO and WT mice fed a standard diet (SD) or a high-fat diet (HFD) (n = 10–16 mice per group). **B)** Macroscopic appearance of livers from 27-week-old LTA$_4$H-KO and WT mice fed the HFD. **C)** Liver masses of LTA$_4$H-KO and WT mice (n = 6–9 mice per group). **D, E)** Representative images of hematoxylin and eosin (H&E)-stained histological sections from LTA$_4$H-KO and WT mice fed the HFD until 27 weeks of age (D, liver; E, BAT; upper panels). Quantification of the lipid droplet area ratio (lower left) and lipid droplet size (lower right) (n = 6–9 mice per group). Scale bars, 100 μm. **F)** Body composition of 12-week-old control (Ctrl; WT and LTA$_4$H-hetero) and LTA$_4$H-KO mice fed the SD (n = 9–10 mice per group). **G)** Body composition of LTA$_4$H-KO and WT mice fed the HFD until 12 weeks of age (n = 7–10 mice per group). Graphs represent means ± SEMs **(A, C, and D–G)**. Statistical analysis was performed using two-way ANOVA **(A)** or unpaired Student's t-test **(C–G)**: ****, $p < 0.0001$; ***, $p < 0.001$; **, $p < 0.01$; *n.s.*, not significant.

Figure 2. LTA$_4$H deficiency protects mice from diet-induced obesity by stimulating energy expenditure. A) Food intake by LTA$_4$H-KO and WT mice fed the HFD at 8–11 weeks of age (n = 6 mice per group). **B)** Residual energy in the feces of LTA$_4$H-KO and WT mice fed the HFD (n = 3 mice per group). **C)** Representative images of H&E-stained small intestinal sections from LTA$_4$H-KO and WT mice fed the HFD until 12 weeks of age. Scale bars, 100 μm. **D)** Energy expenditure and locomotor activity of 12-week-old Ctrl and LTA$_4$H-KO mice fed the SD (n = 9–10 mice per group). **E)** Energy expenditure and locomotor activity of LTA$_4$H-KO and WT mice fed the HFD until 12 weeks of age (n = 7–10 mice per group). The graphs show the means ± SEMs **(A, D and E)** and means ± SDs **(B)**. Statistical analysis was performed using two-way ANOVA **(A)** or unpaired Student's t-test **(B, D and E)**: *, $p < 0.05$; *n.s.*, not significant.

Figure 3. LTA$_4$H deficiency stimulates BAT thermogenesis through neuroendocrine axis. A, B) Body mass gain of mice that had undergone bone marrow transplantation and

the HFD feeding between 15 and 27 weeks of age. LTA_4H-KO and WT mice (Ly 5.2) reconstituted with WT (Ly 5.1) bone marrow (A, n = 9–12 mice per group), and WT mice (Ly 5.1) reconstituted with WT or LTA_4H-KO (Ly 5.2) bone marrow (B, n = 8–9 mice per group), were studied. **C)** Expression of brown adipocyte-specific marker genes in interscapular BAT from LTA_4H-KO and WT mice fed the HFD until 24 weeks of age. Gene expression relative to that of *Actb* is shown (n = 4 mice per group). **D)** Expression of *Ucp1* in BAT from LTA_4H-KO and WT mice fed the SD or HFD until 12 weeks of age. The relative expression of *Ucp1* to *Rps18s* is shown (n = 4 mice per group) **E)** Expression of brown adipocyte-specific marker genes in primary brown adipocytes harvested from LTA_4H-KO and WT mice at 8 weeks of age. The expression relative to that of *Rps18s* is shown (n = 3). **F)** Time course of *Ucp1* expression in primary brown adipocytes harvested from LTA_4H-KO and WT mice before and after isoproterenol stimulation (n = 7 for every time point). **G)** Plasma TSH, T4, and T3 concentrations in HFD-fed LTA_4H-KO and WT mice (n = 8–9 mice per group) **H)** 24-hour urinary noradrenaline excretion by LTA_4H-KO and WT fed the SD or HFD (n = 8–9 mice per group). The graphs show the means ± SEMs **(A, B, and F–H)** and means ± SDs **(C–E)**. Statistical analysis was performed using two-way ANOVA **(A, B and F),** unpaired Student's t test **(C, E and G)**, paired Student's t test **(H)**, or one-way ANOVA **(D)**: ****, $p < 0.0001$; ***, $p < 0.001$; **, $p < 0.01$; *, $p < 0.05$; *n.s.*, not significant.

Figure 4. BLT1-KO mice do not show the lean phenotype. A) Growth curve of BLT1-KO mice and WT mice fed the SD or HFD (n = 24–31 mice for the SD group; n = 8–10 mice for the HFD group). **B, C)** Representative images of H&E-stained histological sections (B, liver; C, BAT) from 29-week-old BLT1-KO and WT mice fed the HFD. Scale bars, 100 μm. **D)** Body composition of BLT1-KO and WT mice fed the HFD until 12 weeks of age (n = 7 mice per group). Graphs represent means ± SEMs **(A and D)**. Statistical analysis was performed using two-way ANOVA **(A)** or unpaired Student's t test **(D)**: *n.s.*, not significant.

Figure 1

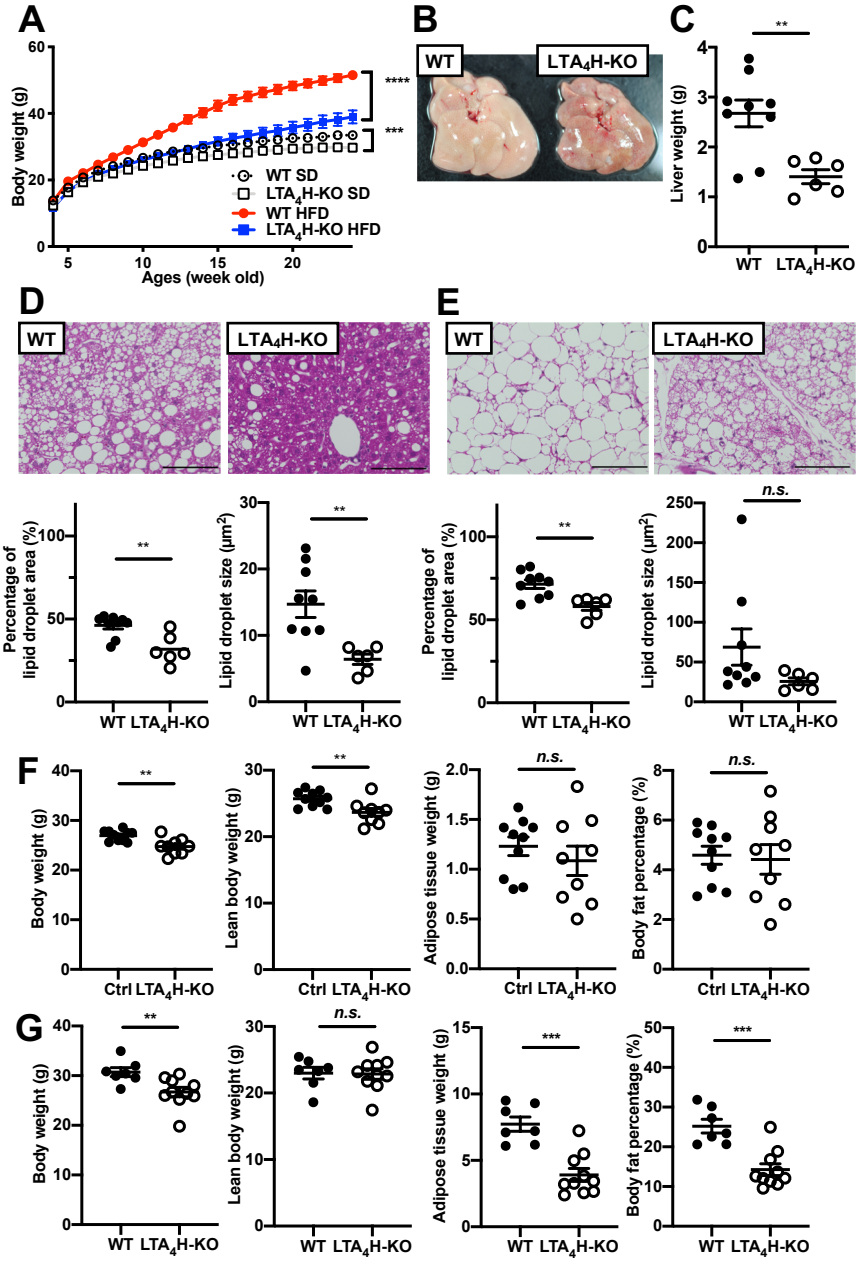
A
Body weight (g)
Ages (week old)
WT SD
LTA4H-KO SD
WT HFD
LTA4H-KO HFD
****
***
B
WT
LTA4H-KO
C
Liver weight (g)
WT
LTA4H-KO
D
E
Percentage of lipid droplet area (%)
Lipid droplet size (μm2)
n.s.
F
Body weight (g)
Lean body weight (g)
Adipose tissue weight (g)
Body fat percentage (%)
Ctrl
G

Figure 2

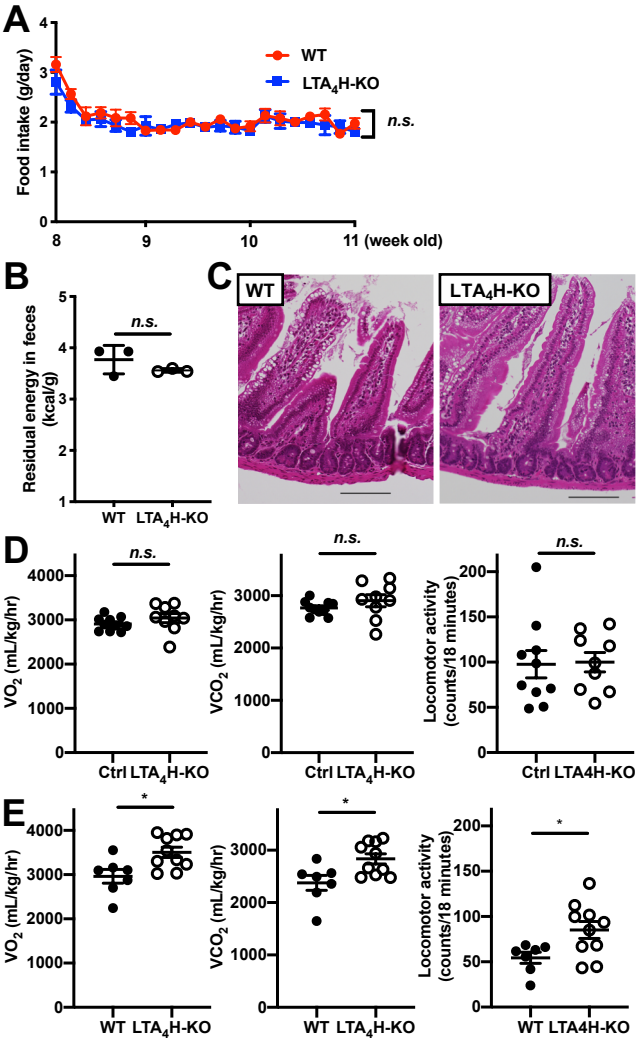
A
Food intake (g/day)
WT
LTA4H-KO
n.s.
8
9
10
11 (week old)
B
Residual energy in feces (kcal/g)
n.s.
WT
LTA4H-KO
C
WT
LTA4H-KO
D
VO2 (mL/kg/hr)
VCO2 (mL/kg/hr)
Locomotor activity (counts/18 minutes)
n.s.
Ctrl
LTA4H-KO
LTA4H-KO
E
*
WT
LTA4H-KO

Figure 3

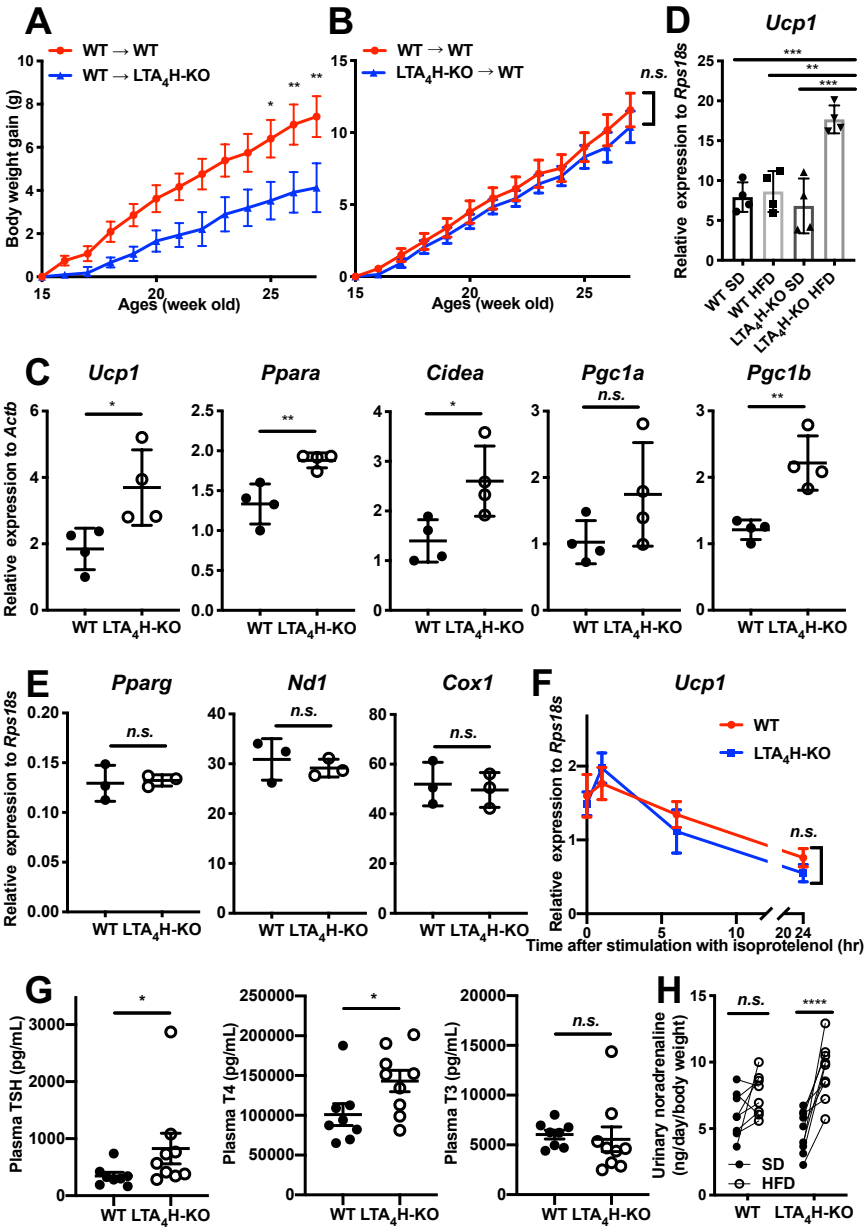
A
WT → WT
WT → LTA4H-KO
Body weight gain (g)
Ages (week old)
B
WT → WT
LTA4H-KO → WT
n.s.
Ages (week old)
D
Ucp1
Relative expression to Rps18s
WT SD
WT HFD
LTA4H-KO SD
LTA4H-KO HFD
C
Ucp1
Ppara
Cidea
Pgc1a
Pgc1b
Relative expression to Actb
WT LTA4H-KO
E
Pparg
Nd1
Cox1
Relative expression to Rps18s
n.s.
F
Ucp1
WT
LTA4H-KO
Relative expression to Rps18s
Time after stimulation with isoprotelenol (hr)
G
Plasma TSH (pg/mL)
Plasma T4 (pg/mL)
Plasma T3 (pg/mL)
H
Urinary noradrenaline (ng/day/body weight)
SD
HFD
WT
LTA4H-KO

Figure 4

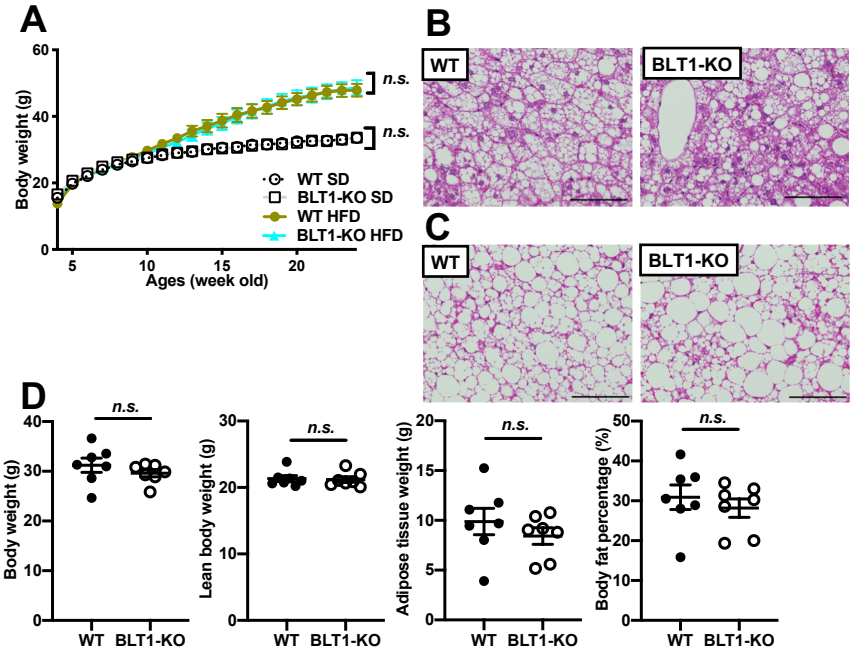
A
Body weight (g)
Ages (week old)
n.s.
n.s.
WT SD
BLT1-KO SD
WT HFD
BLT1-KO HFD
B
WT
BLT1-KO
C
WT
BLT1-KO
D
Body weight (g)
Lean body weight (g)
Adipose tissue weight (g)
Body fat percentage (%)
n.s.
WT
BLT1-KO

Supplemental Figure

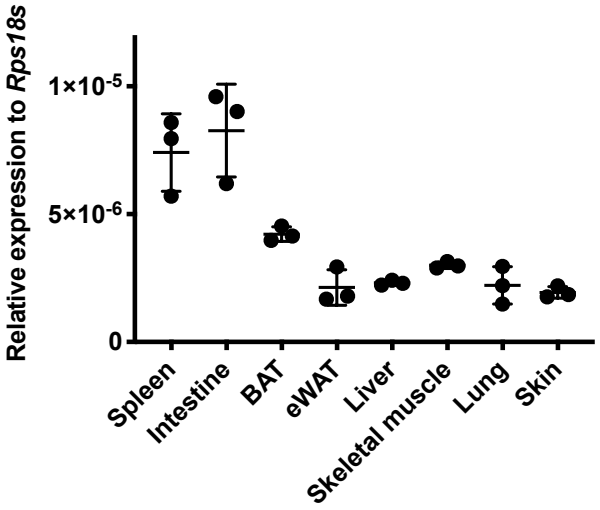

Figure S1. Gene expression of *Lta4h* in various tissues
Expression of the *Lta4h* gene in tissues from 10-week-old WT mice. Expression is shown relative to that of *Rps18s* (*n* = 3 per mice).

Supplemental Figure

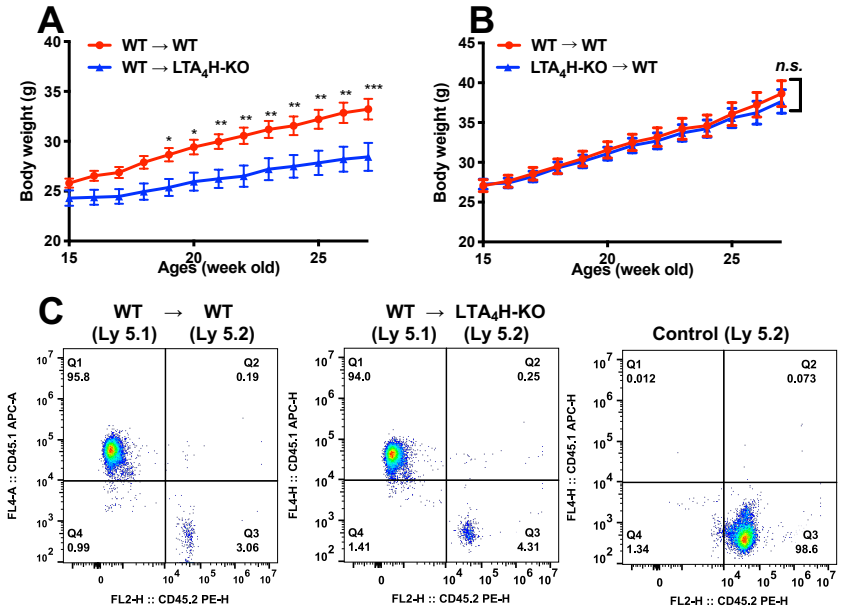

Figure S2. LTA_4H expressed in non-hematopoietic cells contributes to the metabolic phenotype

A, B) Growth curves of bone marrow-transplanted mice fed the HFD. LTA_4H-KO and WT mice (Ly 5.2) reconstituted with WT (Ly 5.1) bone marrow cells (A, *n* = 9–12 mice per group), and WT mice (Ly 5.1) reconstituted with WT or LTA_4H-KO (Ly 5.2) bone marrow (B, *n* = 8–9 mice per group), were studied. The body masses of these mice were measured between 15 and 27 weeks of age. **C)** Representative flow cytometric data for peripheral blood leukocytes from WT (left) and LTA_4H-KO (Ly 5.2) mice (middle) transplanted with WT bone marrow cells (Ly 5.1). The right panel shows the leukocytes from WT (Ly 5.2) mice.